UNIVERSAL MODE OPERATION OF THE BESSY II UE112 APPLE UNDULATOR

J. Bahrdt, W. Frentrup, A. Gaupp, M. Scheer, Helmholtz-Zentrum Berlin für Materialien und Energie, Berlin, Germany

Abstract

The UE112 APPLE undulator operated at BESSY II covers the low photon energies down to the visible regime. Below 100eV the state of polarization is significantly modified by the optical components of the beamline. Moving three magnet rows of the APPLE undulator (universal mode) any state of polarization can be produced by the undulator which permits the compensation of the beamline effects. The dynamic multipoles in the universal mode have to be compensated for a transparent operation. An analytic model of the multipoles has been developed and compared to measurements. A real time compensation scheme is presented.

INTRODUCTION

The user demands a specific state of polarization at the end of the beamline. At low energies the beamline components modify the polarization of the undulator radiation. These energy dependent effects are strongly correlated to the contamination of the optics and they may change over time. Nahon discusses the compensation of the beamline effects with an appropriate setting of the electromagnetic undulator OPHELIE [1]. OPHELIE is a system of two electromagnetic planar undulators rotated 90° with respect to each other where one of them is movable in longitudinal direction. Thus, OPHELIE can generate any state of polarization. In storage rings a large horizontal aperture is required for injection and short period devices have to be built as planar devices. Thus, the two undulator concept can not be applied. In the following we describe a new operation mode of APPLE undulators which permit the production of any arbitrary state of polarization. APPLE II undulators are the preferred sources for variable polarization in many facilities due to the high magnetic field. The low electron energy of BESSY II and the large period length of the UE112 require a careful analysis of the dynamic multipoles and compensation schemes have to be elaborated.

THE APPLE UNIVERSAL MODE

The flexible design of an APPLE undulator with four magnet rows permits various modes of operation. Moving two diagonal rows in the same direction produces elliptically polarized light. Shifting the same rows in opposite direction delivers linearly polarized with variable inclination angle between 0° and 90°. The range can be switched to 90°-180° by moving the other two rows. An energy tuning can be accomplished as well by moving three rows independently which does not require a gap drive. The UE44 built at the PSI [2] is a fixed gap APPLE device of this kind. In the following we will discuss a new mode of APPLE operation, the universal mode, which permits the generation of arbitrary polarization.

The three parameters energy, ellipticity and inclination of the polarization ellipse require three independent knobs for adjustment which can be represented as:

$$\begin{aligned} pp &= (a_1 + a_2)/2 - (a_3 + a_4)/2 \\ pa &= |a_1 - a_2|/2 - |a_3 - a_4|/2 \\ pe &= (a_1 + a_3)/2 - (a_2 + a_4)/2 \end{aligned} \quad (1)$$

The unit of the four row phases $a_1 - a_4$ (see figure 1) and the parameters pp, pa, pe is the undulator period length λ. Since the UE112 has a gap drive we do not need the variable pe which is used in an adjustable phase undulator for energy tuning. Based on this parametrization the performance of the undulator can be represented with contour plots as given in figure 2.

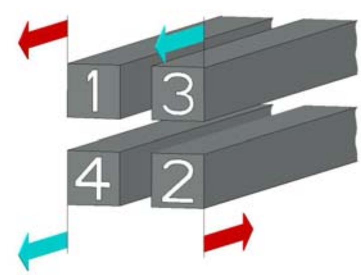

Figure 1: The variables *pp* (blue) and *pa* (red) define the distance of parallel motion (rows 3, 4) and antiparallel motion (rows 1, 2), respectively. The device is operated with an arbitrary combination of *pp* and *pa*.

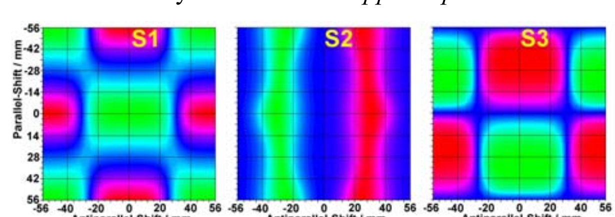

Figure 2: Contour plot of the Stokes parameter S1, S2 and S3 versus the phase parameters $pp \times \lambda$ (vertical axis) and $pa \times \lambda$ (horizontal axis).

The complicated 3D field of an APPLE requires a careful compensation of the dynamic multipoles in particular for long period lengths and low electron energies. In the elliptical mode passive compensation schemes are possible [3-4]. The inclined mode requires an active compensation which has already been implemented at the BESSY UE112 [5]. Since the parameter space in the universal mode is larger by one dimension as compared to the elliptical or the inclined mode a detailed commissioning of all possible modes is not possible and a feed forward compensation of the dynamic multipoles based on analytic expressions is essential. E.g.: The UE112 APPLE produces dynamic multipoles as high as 3Tmm which change with gap and row phase. Flat wires have been glued onto the vacuum chamber to compensate for these multipoles [5]. For the elliptical and the inclined mode the correction currents are symmetric with respect to the undulator axis which permits the coupling of diagonal wires. This limits the number of power supplies to 14. In the universal mode the loss of symmetry may require up to 28 power supplies. In the next section we describe a fast method for the evaluation of the dynamic effects which is suited for real time compensation algorithm.

ANALYTIC MODEL

An analytic description of the fields of an APPLE type undulator has been presented in [6]. The model is based on a Fourier expansion of the fields of two vertically oriented magnet rows and an extrapolation to a four row symmetry. These expressions have been used to derive analytic expressions for the dynamic multipoles making use of eq.2 [7]:

$$\theta_{x/y} = -\frac{1}{(B\rho)^2}\int\left\{\int B_x dz' \cdot \int \frac{\partial B_x}{dx/y} dz' + \int B_y dz' \cdot \int \frac{\partial B_y}{\partial x/y} dz'\right\} dz \quad (2)$$

Field integrals of shims have been described as well in [6]. So far, only the elliptical mode and inclined mode has been studied. In the following we describe a shim model for the universal mode. The field integrals of the L-shims have been evaluated with RADIA [8] on the grid given in table 1.

pp	0	-0.125	-0.250	-0.375	-0.500
pa	0	0.125	0.250	0.375	0.500

Table 1: The table contains the phases for the evaluation of the shim field integrals. The unit is one period length.

The horizontal and vertical field integral components have been decomposed into cos- and sin-functions yielding the coefficients $c_{xi}(s_1, s_2)$ and $s_{xi}(s_1, s_2)$ for the horizontal components and $c_{yi}(s_1, s_2)$ and $s_{yi}(s_1, s_2)$ for the vertical components, respectively. Using these coefficients the shim field integrals for a given shift combination (s_1, s_2) can be evaluated from eq. 3. The coefficients have been evaluated at smallest gap since the dynamic multipoles decay quadratic with gap. An exponential factor accounts for the difference to the reference gap. This assumes a linear superposition of the effects of both magnet girders which is accurate within a few percent. Coefficients for other phases than listed in table 1 are interpolated.

Using this model in combination with the main field model we have a fully analytic description of the undulator. Based on these expressions we can easily derive analytic equations for the tune shifts in the midplane. In the next sections these values will be compared to measured tune shifts.

$$\begin{aligned}
&\widetilde{B}_x = \sum_{i=1}^{n} e^{-k_i \Delta gap/2} \cdot (\\
&\cos(k_i x)(-A4 \cdot \exp(-k_i y) + A2 \cdot \exp(k_i y)) + \\
&\sin(k_i x)(A1 \cdot \exp(-k_i y) - A3 \cdot \exp(k_i y))) \\
&\widetilde{B}_y = \sum_{i=1}^{n} e^{-k_i \Delta gap/2} \cdot (\\
&\cos(k_i x)(A1 \cdot \exp(-k_i y) + A3 \cdot \exp(k_i y)) + \\
&\sin(k_i x)(A4 \cdot \exp(-k_i y) + A2 \cdot \exp(k_i y))) \\
&k_i = i \cdot (2\pi / \lambda_1) \\
&A1 = (c_{yi} + s_{xi})/2 \\
&A2 = (s_{yi} + c_{xi})/2 \\
&A3 = (c_{yi} - s_{xi})/2 \\
&A4 = (s_{yi} - c_{xi})/2
\end{aligned} \quad (3)$$

MEASUREMENTS

Horizontal and vertical tune shifts have been measured for a gap of 24mm and row phase values given in table 1. The measurements have been performed for a transversally displaced electron beam of -8, -6, -4, -2, 0, 2, 4, 6 mm. After the electron beam has been displaced at largest undulator gap the orbit has been corrected and the tunes have been set to the nominal values for largest gaps and phases equal zero. Then the gap has been closed to 24mm with running closed orbit feed back and the tunes have been measured for the phase settings of table 1. For each beam displacement the corresponding tune for *pp* = *pa* = 0 have been subtracted.

Figure 3 gives the results for electron beam displacements of 4mm and -4mm. The tune asymmetry for the values *pa* = 0.125, 0.250 and 0.375 are due to the asymmetry of the magnetic field in this operation mode. Figure 3 shows a good agreement between measurement and simulation for displacements of ±4mm. Without any fitting procedure the tunes are well reproduced within 20%. The data for all transverse displacements are summarized in figures 4 and 5. The differences between measurement and simulation (red distribution) are significantly smaller than the measured tune shifts. The deviations are due to the simple model which is based on nominal values. It is expected that the differences will be even smaller in a refined model which will be based on the following steps:

- Fitting of the total strength of the L-shims.
- Regarding also the small Fe shims (so far only the large L-shims are included).
- Fitting of the betatron function.
- Fitting of the linear response of the beam position monitors; the nonlinear part is extrapolated from the steerer currents applied for the electron displacement.

- Fitting of the horizontal position of the electron beam with respect to the undulator axis.

The refined model including the five fitted parameters is still scalable in gap and row phases due to the analytical ansatz. Thus, the evaluation of the dynamic field integrals and the corresponding current setting for the flat wires can be done online.

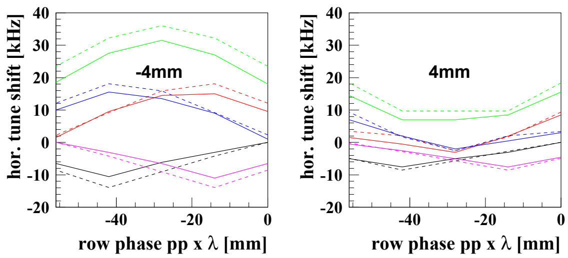

Figure 3: Horizontal tune shifts of the BESY II UE112 versus row phase *pp* as defined in figure 1. The colours correspond to values of *pa* = 0 (black), 0.125 (red), 0.250 (green), 0.375 (blue), 0.500 (magenta). Solid lines: measurements, dashed lines: simulations.

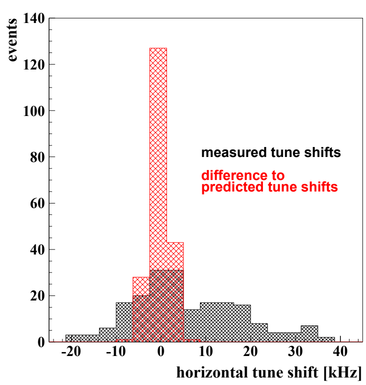

Figure 4: Measured horizontal tune shifts (black) and deviation to simulation (red) of the BESSY II UE112.

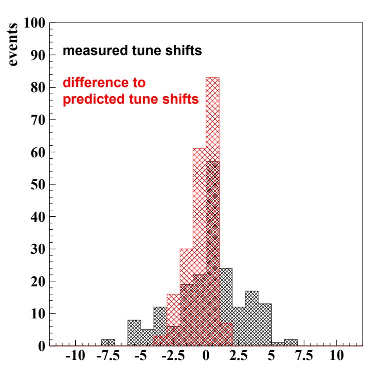

Figure 5: Measured vertical tune shifts (black) and deviation to simulation (red) of the BESSY II UE112.

Based on the evaluated dynamic multipoles for the smallest gap and for the 25 phase parameters as listed in table 1 the compensation currents for the flat wires installed at the UE112 chamber have been fitted with a linear algorithm. For each combination of *pp* and *pa* the residuals (rms-values) within a horizontal range of ±25mm are below 0.003Tmm. The highest current amounts to 25A. So far the wires (thickness of 300μm) have been tested with 16A. If 25A will lead to intolerable heat problems, thicker wires can be used. The data have been fitted with a constant offset of up to 5Gm which can be applied with wide air coils. Without compensating this offset the compensation currents would higher and the residuals would increase to 0.018Tmm with large fluctuations along the transverse axis.

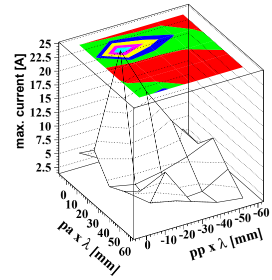

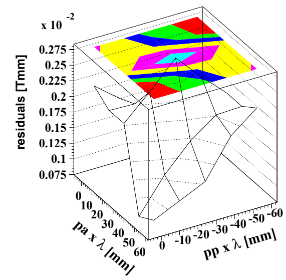

Figure 6 (left): Maximum compensation currents. Figure 7 (right): Residuals of field integrals with compensation for various combinations of *pp* and *pa*.

CONCLUSION

The tune shifts can be evaluated fast and with high accuracy. Appropriate correction currents can be derived by solving a set of linear equations. Thus, the evaluation of the correction currents can be done within a time frame which is compatible with an online compensation scheme and the generation of feed forward tables will not be required.

REFERENCES

[1] L. Nahon, C. Alcaraz, Applied Optics, Vol 43, No. 5 (2004) pp1024-1037.

[2] T. Schmidt, D. Zimoch, AIP-Proceedings of the 9th Int. Conference on Synchr. Rad. Instr., Daegu, South-Korea, pp 404-407.

[3] J. Chavanne et al., Proceedings of the EPAC 2000, Vienna, Austria, pp 2346-2348.

[4] J. Bahrdt, W. Frentrup, A. Gaupp, M. Scheer, AIP-Proceedings of the 9th Int. Conference on Synchr. Rad. Instr., Daegu, South-Korea, 2006, pp 315-318.

[5] J. Bahrdt, W. Frentrup, A. Gaupp, M. Scheer, G. Wuestefeld, Proceedings of the EPAC 2008, Genoa, Italy, pp 2222-2224.

[6] J. Bahrdt, M. Scheer, G. Wuestefeld, Proceedings of the EPAC 2006, Edinburgh, Scotland, pp 3562-3564.

[7] P. Elleaume, Proceedings of the EPAC 1992, Berlin, Germany, pp 661-663.

[8] O. Chubar, P. Elleaume, J. Chavanne, Journal of Synchrotron Radiation (1998) 5, pp 481-484.